Social Cognitive and Affective Neuroscience Advance Access published May 17, 2011

doi:10.1093/scan/nsr018 SCAN (2011) 1 of 9

Spontaneous resting-state BOLD fluctuations reveal persistent domain-specific neural networks

W. Kyle Simmons[1,2] and Alex Martin[1]

[1]Laboratory of Brain and Cognition, National Institute of Mental Health, Bethesda, Maryland and [2]Laureate Institute for Brain Research, Tulsa, Oklahoma, USA

Resting-state functional connectivity MRI (rs-fcMRI) analyses have identified intrinsic neural networks supporting domain-general cognitive functions including language, attention, executive control and memory. The brain, however, also has a domain-specific organization, including regions that contribute to perceiving and knowing about others (the 'social' system) or manipulable objects designed to perform specific functions (the 'tool' system). These 'social' and 'tool' systems, however, might not constitute intrinsic neural networks *per se*, but rather only come online as needed to support retrieval of domain-specific information during social- or tool-related cognitive tasks. To address this issue, we functionally localized two regions in lateral temporal cortex activated when subjects perform social- and tool conceptual tasks. We then compared the strength of the correlations with these seed regions during rs-fcMRI. Here, we show that the 'social' and 'tool' neural networks are maintained even when subjects are not engaged in social- and tool-related information processing, and so constitute intrinsic domain-specific neural networks.

Keywords: social cognition; tools; resting-state functional connectivity; posterior superior temporal sulcus; middle temporal gyrus

INTRODUCTION

Recently, there has been heightened interest in identifying intrinsic neural functional connectivity by measuring correlations among brain regions in the slow, spontaneous fluctuations that characterize the blood oxygenation level dependent (BOLD) functional magnetic resonance imaging (fMRI) signal. These so-called resting-state functional connectivity MRI (rs-fcMRI) analyses have been used to map large polysynaptic cortical networks distributed throughout the brain. Although this method is perhaps most associated with efforts to study the brain's 'Default Network' (Raichle *et al.*, 2001; Greicius *et al.*, 2003; Fox *et al.*, 2005), evidence has accumulated from rs-fcMRI that there exist other large-scale intrinsic neural networks supporting traditional psychological functions such as language (Cordes *et al.*, 2000; Hampson *et al.*, 2002), attention (Fox *et al.*, 2006), visual perception (Cordes *et al.*, 2000), motor functioning (Biswal *et al.*, 1995), executive control (Seeley *et al.*, 2007; Vincent *et al.*, 2008) and memory (Vincent *et al.*, 2006).

Extensive cognitive, developmental, neuropsychological and neuroscience literatures demonstrate, however, that the brain is not organized only in terms of domain-general psychological/cognitive distinctions that transcend primary sensory and motor systems (e.g. language, memory, attention, etc.). Rather, the brain also has a domain-specific cognitive organization with systems specialized for processing specific classes of information (Hirschfeld and Gelman, 1994; Caramazza and Shelton, 1998). Prominently included in the list of domain-specific systems are the 'social-cognitive system'—including regions involved in perceiving and knowing about others—and a system for perceiving and knowing about manipulable objects designed to perform specific functions—in other words 'tools' [for reviews see (Caramazza and Shelton, 1998; Martin, 2007; Martin and Simmons, 2008)].

Lesion and neuroimaging evidence, both in monkeys and humans, supports the existence of dissociable domain-specific social-cognitive and tool systems (Lewis, 2006; Frith, 2007). Importantly, the constituent brain regions within each system appear to store and represent types of information (or properties) that are salient for social agents and tools (Martin, 2007). For example, functional neuroimaging studies often report that when individuals engage in social cognition, a collection of regions co-activate, including the posterior superior temporal sulcus (pSTS) to represent information about biological motion (Beauchamp *et al.*, 2002, 2003; Deen and McCarthy, 2010; Grossman *et al.*, 2010), the lateral portion of the fusiform gyrus to represent information about faces and bodies (Puce *et al.*, 1996; Kanwisher *et al.*, 1997; Schwarzlose *et al.*, 2005; Kanwisher and Yovel, 2006), the posterior cingulate and precuneus to facilitate social perspective taking and representation of the self (Cavanna and Trimble, 2006; Andrews-Hanna *et al.*, 2010b), the insula to represent visceral-emotive responses to social stimuli (von dem Hagen *et al.*, 2009; Bird *et al.*, 2010), the amygdala for detecting emotionally salient social stimuli (Adolphs and Spezio, 2006; Adolphs, 2010), the

Received 22 December 2010; Accepted 1 March 2011

The authors would like to thank Mark Reddish and Seth Kallman for assistance in data collection in preparing manuscript tables. The authors would also like to thank Steve Gotts, Avniel Ghuman and Pat Bellgowan for helpful discussions.

This work was supported by the National Institute of Mental Health Division of Intramural Research, National Institutes of Health.

Correspondence should be addressed to Kyle Simmons, Laureate Institute for Brain Research, 6655 South Yale Avenue, Tulsa, OK 74136-3326, USA. E-mail: wksimmons@laureateinstitute.org

anterior temporal lobes for the representation of social conceptual knowledge (Simmons and Martin, 2009; Ross and Olson, 2010; Simmons *et al.*, 2010) and the medial prefrontal cortex (mPFC) for social reasoning, including theory of mind (Amodio and Frith, 2006; Frith, 2007).

In contrast to the regions implicated in social cognition, perceiving or thinking about tools is associated with co-activation of a different collection of regions lateralized primarily to the left hemisphere, including the posterior middle temporal gyrus (pMTG) to represent non-biological motion (Beauchamp *et al.*, 2002, 2003), the ventral premotor cortex to store and retrieve general motor programs that form the 'basic vocabulary' of manual movements necessary to manipulate tools (Davare *et al.*, 2006) and the inferior parietal lobe for representing information about the execution of complex gestures associated with tool manipulation (Haaland *et al.*, 2000; Goldenberg and Spatt, 2009).

In the literature cited above, both activations in functional neuroimaging studies and behavioral performance of lesion patients are measured in task contexts that involve thinking about the category. This being the case, it is possible that the 'social' and 'tool' systems are not intrinsic neural networks, but rather only come online as needed to support retrieval of properties shared by category members either explicitly, as in retrieving information during property verification tasks, or implicitly during object recognition and naming. Because the properties shared by social agents or tools, respectively, are so highly correlated with one another (e.g. thinking about a hammer means not only retrieving information in pMTG about how it moves, but also information in ventral premotor cortex about how it is grasped), the co-activation of social- or tool property regions during domain-specific processing tasks tells us little about whether these regions constitute intrinsic, persistent networks in the adult brain. Rather, determining whether these systems are intrinsic neural networks requires assaying these systems outside of social- and tool tasks. Resting-state functional connectivity analyses are ideal for this purpose.

If the co-activation of social- or tool property regions during social- or tool tasks results strictly from the online retrieval of salient properties correlated with social- or tool category membership, then the property regions within the networks should de-couple during rest. As a result, functional connectivity among social- and tool property regions, respectively, should not be apparent within resting-state data. This finding would significantly constrain and weaken domain-specific accounts of social and tool cognition.

Alternatively, if intrinsic connectivity exists among the social- and tool property regions irrespective of what a person is thinking about, each network should be apparent in functional connectivity analyses of data collected during resting-state scans when subjects are not engaged in tool- or social-processing tasks. This finding would significantly strengthen domain-specific accounts of social- and too cognition.

In the present study, we localized regions in the right pSTS and left pMTG active while subjects performed social- and tool conceptual-processing tasks, and then compared the strength of the correlations with these two seed regions during resting state fMRI, both within those same subjects, and in different subjects. We chose the pSTS and pMTG as seed regions because: (i) they are both located in lateral posterior temporal cortex, and so have nearly identical fMRI temporal signal-to-noise characteristics; (ii) they both respond to similar types of visual information, namely motion (either biological or non-biological); and (iii) they both have large literatures supporting their roles within the social–cognitive and tool use neural networks.

Using Pearson correlations in resting-state functional connectivity analyses, here we show that both the 'social–cognitive' and 'tool' neural networks are maintained even when subjects are not engaged in social–cognitive and tool-related information processing. As evidence of the reliability of the findings in this data set (hereafter referred to as the 'System Identification Study'), we then replicated these effects in a separate independent resting-state data set (hereafter referred to as the 'Replication Study').

METHODS

Participants

Twenty-five right-handed, native English-speaking volunteers (14 female; mean age = 25.2 years range, 21–35 years) participated in the System Identification study. Twelve right-handed, native English-speaking volunteers (7 female; mean age = 24.3 years range, 20–32 years) participated in the independent Replication Study. The two sets of subjects in the System Identification and Replication studies were paid for their participation, and all read and signed informed consent documents in accordance with NIH IRB protocols. All subjects completed health questionnaires, and none reported prior head injuries or neurological problems, nor did they report recent use of psychotropic medications.

Experimental design

To localize person- and tool knowledge regions, 12 subjects performed a fact-learning task while undergoing fMRI (resting state data from these same 12 subjects constituted the Replication data set). For greater detail on the task, see (Simmons *et al.*, 2010). In brief, subjects were presented with short sentences, each stating a fact about four unique and novel persons, buildings or hammers. For each entity subjects learned an age, location and usage/occupation fact (e.g. 'Patrick was born in Seattle', 'The Brooks hammer is used to break drywall', etc.), thus learning the same types of information, but about different object domains. Sentences were presented in 18-s blocks, with all three sentences in the block referring to the same entity, each presented for 6 s. There were three fact-learning task scan runs, with all facts about each entity presented in each run. Post-scan memory tests

revealed that memory for the facts was good (mean person-fact recall = 72%, mean tool-fact recall = 65%).

System identification study

To provide an independent data set in which we could evaluate functional connectivity, 25 subjects performed a resting-state scan during which they were instructed to lie still and fixate a centrally located crosshair. To ensure that they remained awake, subjects were instructed to press a button on a handheld response box when they saw the crosshair change color, which occurred very infrequently (mean interchange duration = 60 s, range 30–90 s). The subjects in the System Identification Study did not perform the fact-learning task used to localize the pSTS and pMTG seed regions for the functional connectivity analyses.

Replication study

The same subjects that performed the fact learning pMTG/pSTS localizer study also performed the same resting-state scan as those in the System Identification Study. All resting-state scans were collected prior to the three fact-learning task runs.

Image acquisition

Stimuli were projected onto a screen at head of the scanner and viewed by subjects with a mirror mounted on the head coil. Stimulus presented was controlled using Eprime version 1 (www.pstnet.com).

Imaging parameters during the resting-state scans were identical for both the System Identification and Replication data sets. One hundred and forty echoplanar MR volumes depicting BOLD contrast were collected with a HDx short-bore General Electric 3 Tesla MRI scanner. In each echoplanar image (epi) volume, 42 contiguous 3-mm thick slices were collected in the axial plane, ensuring whole-brain coverage (TE = 27 ms, TR = 3500 ms, flip angle = 90°, voxel size = 2.3 mm × 2.3 mm × 3 mm). Scan parameters during the Fact-Learning task for the System Identification data set were also identical, except that 143 epi volumes were collected in each run. Both before and after epi scanning, MPRAGE structural images were collected (TE = 6 ms, TR = 25 ms, flip angle = 15°, voxel size = 0.9 mm × 0.9 mm × 1.2 mm). A General Electric 8-channel head coil was used for all scanning runs, with a SENSE factor of 2 used to minimize epi distortions while also reducing gradient coil heating over the course of the scan session. See Figure 1 in (Simmons *et al.*, 2010) for representative temporal signal-to-noise ratio maps using these parameters.

fMRI pre-processing

Prior to statistical analyses, image preprocessing was conducted using the AFNI software package (http://afni.nimh.nih.gov/afni). The second MPRAGE anatomical scan was co-registered to the first MPRAGE, and the two were then averaged to produce a single high-quality anatomical image of the subject's brain, which was then aligned to the epi data using AFNIs anatomical-to-epi alignment python script. Next the anatomical scan was warped to Talairach space using an automated algorithm. In both data sets, the first three volumes of each resting-state run were removed and slice time correction was applied to each volume. Motion parameters for the epi time courses were estimated for each volume relative to the third volume of the resting-state scanning run. Next, motion correction and spatial transformation of the epi data to Talairach atlas space were implemented in a single image transformation step, with interpolation to a new resolution of $1 \times 1 \times 1\,mm^3$. The epi data were then smoothed with a 6 mm full-width half-max Gaussian kernel, and signal intensity at each time point was normalized to reflect the percent signal change from the voxel's mean signal time course.

fMRI statistical analyses

Functional connectivity analyses were implemented on the subjects' resting-state scanning run. The seed voxels for the social–cognitive and tool use systems in the pSTS and pMTG were determined by the peak *t*-values identified in the person > hammer and hammer > person contrasts, respectively, from the group analysis of the Fact-Learning task data. Based on these contrasts, the pSTS seed voxel was located at 43, −59, 8 and the pMTG seed voxel was located at −50, −56, −2. The posterior cingulate seed voxel used in the comparison of the social–cognitive and default networks was located at −2, −36, 37. This voxel has been previously identified in rs-fcMRI analyses as the peak posterior cingulate voxel within the task-negative or 'Default Network' (Fox *et al.*, 2005).

Although many recent resting-state functional connectivity studies have rightfully used innovative statistical modeling techniques such as graph theory and small-world network analyses, it was possible to achieve the aims of the present study using a simple combination of correlations and paired-sample *t*-tests. The connectivity analyses proceeded as follows. At the subject-level, multiple regression was used to model the run's signal mean, linear, quadratic and cubic signal trends, as well as six motion parameter regressors. In addition, the average signal time course from the subject's ventricles was included to further account for global signal changes. The residual time course for each voxel was then used in the subsequent analyses. Time course residuals for the pSTS, pMTG and posterior cingulate seed voxels were then used as predictors in separate regression analyses to produce a map of the correlations (*r*-values) between each voxel in the brain and the given seed voxel. Next, these *r*-values were converted to *Z*-values using Fisher's *r*-to-*Z* transformation.

To test the domain specificity of the two circuits, it is not enough to simply demonstrate reliable correlations in the spontaneous BOLD fluctuations of regions in the social or tool systems and the right pSTS and left pMTG seeds, respectively. Rather, a claim of domain specificity requires

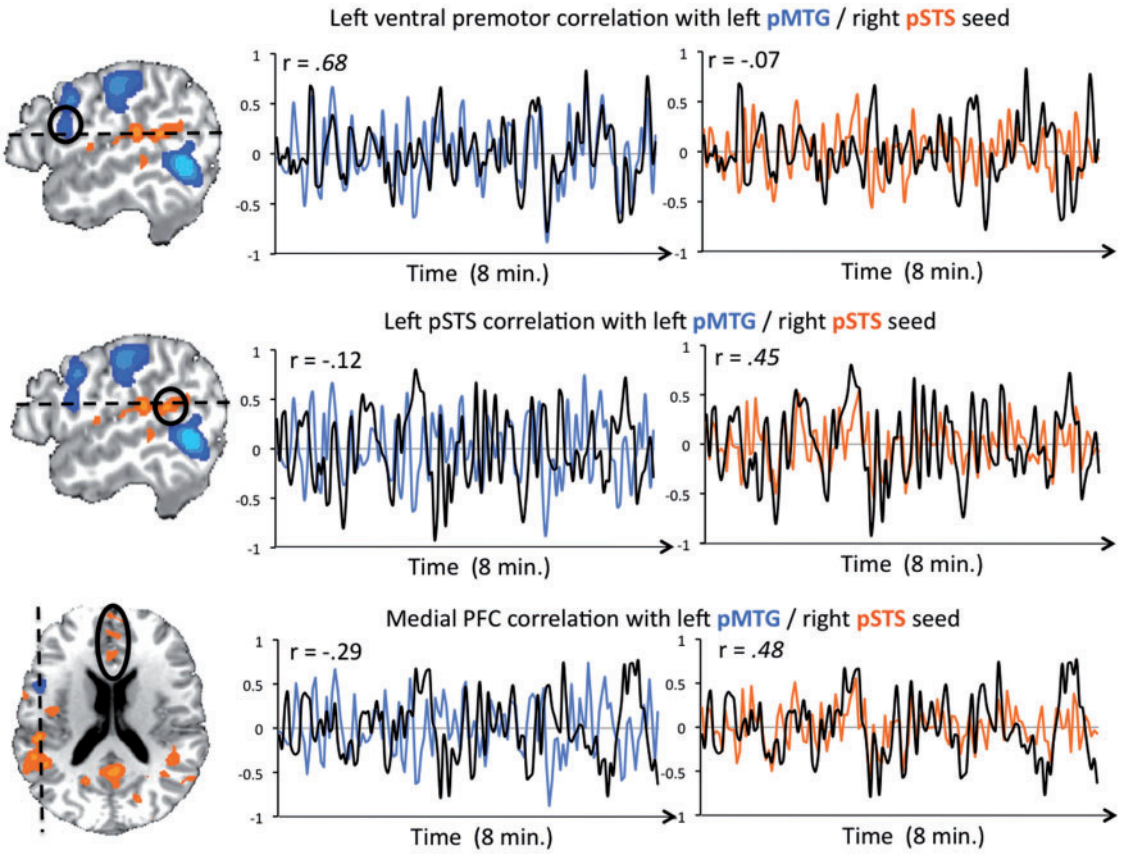

Fig. 1 Resting-state time course graphs illustrating correlated spontaneous BOLD fluctuations in an individual participant. The black lines in the graphs indicate the BOLD activity time courses across the 8-min resting-state scan at the left ventral premotor cortex (top), left pSTS (middle) and medial PFC (bottom). Black circles on the adjacent brain images indicate the locations of the target regions from which these signals were extracted. The locations of the seed voxels are not shown, although the images do show regions of differential connectivity in the left pMTG and right pSTS that are adjacent to the seed voxels. The colors on the brain maps indicate regions exhibiting differential functional connectivity to either the pMTG (cool colors) or pSTS (warm colors), with $P < 0.005$. The blue and orange lines in the graphs show the corresponding time courses at the left pMTG ('tool') and right pSTS ('social') seed voxels, respectively. The time course graphs are presented here for expository purposes to help the reader understand the analyses—namely that differential functional connectivity assesses whether a voxel is reliably more correlated with one seed region than another. The reader should note that the values in these specific graphs are overdetermined because we selected which voxels to plot by first testing for regions exhibiting differential functional connectivity to the pSTS/pMTG. The dashed lines across each of the individual brain images indicate the slice locations of the other brain images depicted in the figure. The *y*-axes on the graphs indicate percent signal change from signal baseline.

demonstrating 'differential' functional connectivity: that spontaneous BOLD fluctuations in regions implicated in social cognition are statistically more correlated with the right pSTS seed than the left pMTG seed, and spontaneous BOLD fluctuations in regions implicated in tool cognition are statistically more correlated with the left pMTG seed than the right pSTS seed (Figure 1). To this end, the subjects' *Z*-maps were included in a random effects paired-sample *t*-test to identify voxels exhibiting reliable differences across subjects between the *Z*-transformed correlations with the pSTS and pMTG seed voxels. Similarly, a second paired-sample *t*-test was used to identify voxels exhibiting reliable differences between the correlations to the posterior cingulate and left pMTG seed voxels.

For the analysis of the resting-state runs in the System Identification Study, statistical thresholds were corrected for multiple comparisons at the $P < 0.05$ level using cluster size corrections implemented in AFNIs AlphaSim. Given a voxel-wise *P*-value threshold of 0.005, correction for multiple comparisons required cluster sizes greater 1160 mm^3. Because fMRI signal quality is relatively poor within the anterior temporal lobes, and yet there is good reason to predict *a priori* that this region is part of the social–cognitive neurocircuit (Ross and Olson, 2010; Simmons *et al.*, 2010), a small volume correction was applied to the volume of the anterior temporal lobes, defined separately in each hemisphere as all temporal lobe voxels anterior to the limen insula (Insausti *et al.*, 1988). Within this anterior temporal region of interest, correction for multiple comparisons at the 0.05 level was achieved with a voxel-wise $P < 0.005$ and a cluster size > 304 mm^3. Finally, given that the Replication Study data set had fewer subjects, and functional connectivity analyses within this data set was intended to test the replicability of findings from the System Identification Study (which employed corrected statistics), the functional connectivity analysis of resting-state data in

the Replication Study employed a somewhat less stringent statistical threshold, with $P < 0.005$ and a cluster size threshold of 476 mm^3 (equivalent to 30 voxels at scan resolution).

To evaluate the overlap between the social–cognitive and default networks in the System Identification Study, conjunction analyses were performed to identify voxels present in both the pSTS > pMTG and posterior cingulate > pMTG statistical contrast maps. Because it is possible that small areas of intersection between clusters from the two maps could be induced by spatial smoothing and resampling, we applied a small cluster-size threshold of at least 10 voxels on all areas of conjunction.

See the Supplementary Materials for a description of how the Fact Learning Task functional localizer data were analyzed.

RESULTS

System identification study

Differential functional connectivity was observed between the left pMTG and regions frequently implicated in tool-related cognition, including the left ventral premotor cortex, the inferior parietal cortex bilaterally and the pMTG on the right (Figures 1 and 2 and Supplementary Table S1). In other words, spontaneous BOLD fluctuations in these regions were not simply reliably correlated with the pMTG seed, but were in fact reliably more correlated with the pMTG seed than with the pSTS seed. In addition, differentially correlated resting-state spontaneous BOLD fluctuations were also observed between the left pMTG and the superior parietal lobe on the right, dorsal middle frontal gyrus on the left and with the inferior frontal gyrus bilaterally. The inferior frontal gyrus clusters were located in nearly exactly homologous regions in the two hemispheres, and ~2.5 cm anterior to the left hemisphere region of correlated activity in the ventral premotor cortex.

In contrast to the connectivity profile of the pMTG, the pSTS exhibited differential connectivity with regions frequently implicated in social–cognition. The right pSTS seed exhibited differential functional connectivity with the contralateral pSTS and middle occipital gyrus, the right posterior fusiform, the right anterior temporal lobe, the right posterior insula and the medial prefrontal cortex and posterior cingulate. Another area of differential functional connectivity was observed in a region of the right superior temporal sulcus, located anteriorly to the seed region, which has often been reported in studies of famous/familiar face recognition. Finally, differential functional connectivity with the pSTS was observed in the left cuneus and on the midline in the caudate.

A subset of regions showing differential connectivity to the pSTS have previously been implicated in so-called

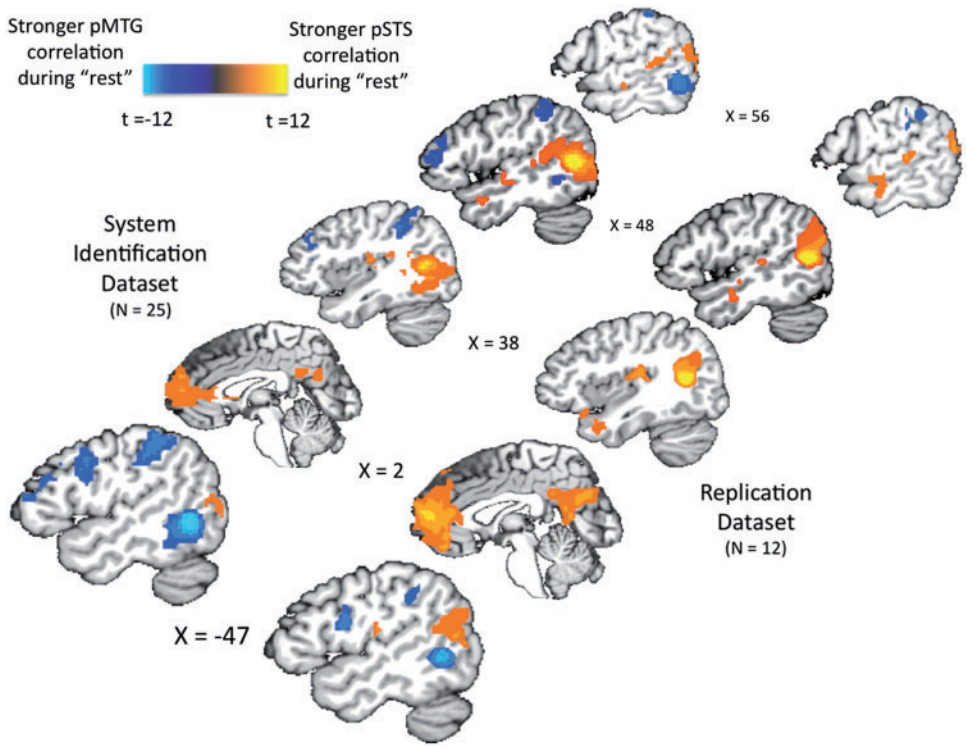

Fig. 2 Random effects group analyses demonstrating regions of differential functional connectivity to the left pMTG ('tool') and right pSTS ('social') seed voxels. Each pair of sagittal brain images shows remarkably similar regions of differential functional connectivity in the System Identification data set (left row, $P < 0.05$ corrected) and Replication data set (right row, $P < 0.005$, cluster size > 476 mm^3). Cool colors indicate higher resting-state BOLD correlations with the left pMTG ('tool') seed voxel than the right pSTS ('social') seed voxel, and warm colors indicate higher correlations with the right pSTS ('social') seed voxel. The exact locations of the seed voxels are not shown in these slices, although the images do show regions of differential connectivity in the left pMTG and right pSTS that are adjacent to the seed voxels.

'default mode' processing (Raichle *et al.*, 2001), and are frequently identified in functional connectivity studies of the default-network (Fox *et al.*, 2005). To examine the relationship between the two systems, we first identified regions of differential connectivity between the left pMTG seed and a posterior cingulate seed identified in previous default network studies (see 'Methods' section). We then identified areas of logical conjunction between the map of regions with greater functional connectivity to the posterior cingulate than to the pMTG, and the map of regions with greater functional connectivity to the pSTS than to the pMTG (Supplementary Table S2). Only three regions exhibited differential connectivity to both the pSTS and the posterior cingulate. The medial prefrontal cortex (primarily anterior cingulate gyrus), the posterior cingulate gyrus and a region of the right supramarginal gyrus, ~1.5 cm dorsal and lateral to the pSTS seed region. In contrast, the majority of the regions implicated in the social–cognitive network were not part of the default network.

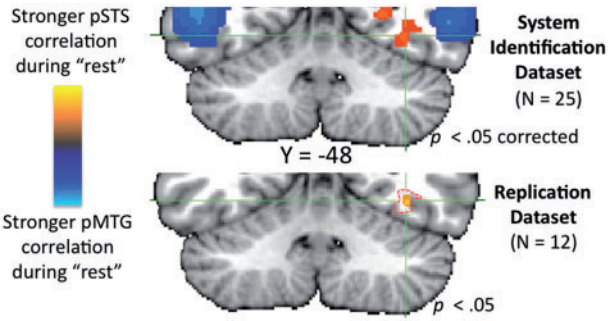

Fig. 3 Evidence of differential fusiform functional connectivity in both data sets. The top coronal image shows a region of the fusiform gyrus that exhibited stronger functional connectivity to the right pSTS ('social') seed voxel than to the left pMTG ('tool') seed voxel ($P < 0.05$ corrected). Although differential functional connectivity was not observed in the fusiform at the threshold prescribed for the Replication data set analyses, it was present at a somewhat less stringent threshold, as illustrated in the bottom coronal image. The bottom image depicts regions of direct overlap between the two data sets within the fusiform gyrus. The red dotted line on the bottom image indicates the spatial extent of the fusiform cluster in the brain image at the top of the figure exhibiting differential functional connectivity to the 'social' seed in the System Identification data set.

Replication data

The results from the replication sample were highly similar to the connectivity profiles observed in the System Identification Study (Figure 2 and Supplementary Table S3). In fact, the strong similarity between the two independent data sets is demonstrated by their whole-brain spatial correlation (Pearson $r = 0.62$). Compared with the pSTS seed, differential function connectivity was observed between the left pMTG and the wider tool use network, including the left ventral premotor cortex and the inferior parietal cortex bilaterally. Areas of direct overlap between the System Identification and Replication data sets were observed in all three regions (Supplementary Table S4).

As with the tool use network, differential connectivity within the social–cognitive network was also observed in the independent Replication data set. When compared with the pMTG seed, differential functional connectivity to the pSTS was again observed in the contralateral pSTS, the right anterior temporal lobe, bilaterally in the posterior insula and the medial prefrontal cortex and posterior cingulate along the midline. As in the System Identification data set, differential functional connectivity was again observed in a region of the right superior temporal sulcus implicated in famous/familiar face recognition. Significantly, the right amygdala, a region often implicated in social cognition but not observed in the System Identification data, was found to exhibit differential functional connectivity with the pSTS in the Replication data set. Finally, differential functional connectivity was also observed in the right cuneus and the left superior frontal gyrus.

Directly overlapping areas exhibiting differential functional connectivity with the pSTS in both the System Identification and Replication data sets were observed bilaterally in the pSTS, the right posterior insula, the medial prefontal cortex and the posterior cingulate (Supplementary Table S4). Direct overlaps were similarly observed at multiple locations along the length of the right middle and superior temporal gyri, and bilaterally in the cuneus. Differential functional connectivity was observed between the fusiform gyrus and the pSTS seed in the System Identification data set using statistics corrected for multiple comparisons, with an overlapping region apparent at a less stringent threshold in the Replication data set ($P < 0.05$) (Figure 3). Any differences between the data sets, such as observing differential functional connectivity between the pSTS and the fusiform in the System Identification data set but not in the Replication data set, may be attributable to the fact that the former had more than twice as many subjects as the latter, and so had much greater statistical power.

DISCUSSION

Large functional neuroimaging and neuropsychological patient literatures demonstrate that dissociable collections of brain regions underlie the perception of, and semantic memory for, social agents and tools. The findings presented here demonstrate that these regions maintain their relative functional intraconnectivity regardless of whether individuals are consciously engaged in social- or tool cognition. In short, the constituent regions within the social- and tool neural networks are persistently coupled to one another, a finding which strongly supports the claims that dissociable domain-specific neural systems support human social and tool cognition (Caramazza and Shelton, 1998; Martin, 2007; Martin and Simmons, 2008).

In the present study, we used a functional localizer task to map two seed regions for subsequent functional connectivity analyses in independent data. One of these seed regions, located in the pSTS, has been implicated in biological

motion perception and social conceptual processing, while the other seed region, located in the pMTG, has been implicated in non-biological motion perception and tool-related conceptual processing (Beauchamp *et al.*, 2002, 2003); for reviews see (Martin and Simmons, 2008). Compared with the pMTG, the pSTS exhibited reliably greater intrinsic functional connectivity to a region of the fusiform gyrus implicated in face and body processing (Kanwisher *et al.*, 1997; Schwarzlose *et al.*, 2005), a region of the posterior cingulate/precuneus implicated in social perspective taking and self-representation (Cavanna and Trimble, 2006; Andrews-Hanna *et al.*, 2010b) and a region in the insula associated with visceral-emotive responses to social stimuli (von dem Hagen *et al.*, 2009; Bird *et al.*, 2010). The pSTS also exhibited greater connectivity with the amygdala, which is frequently activated when subjects are presented with emotionally-salient social stimuli (Adolphs and Spezio, 2006; Adolphs, 2010), and a region of the anterior temporal lobes that has recently been shown to exhibit strong selectivity for social information processing and functional connectivity with other social–cognitive regions (Ross and Olson, 2010; Simmons *et al.*, 2010). In addition, the pSTS was also differentially correlated with a region of the medial PFC that underlies social reasoning, particularly about one's own, and others', mental states (Amodio and Frith, 2006; Frith, 2007; Andrews-Hanna *et al.*, 2010b).

Relative to the pSTS, the pMTG exhibited reliably greater intrinsic functional connectivity to regions previously implicated in tool manipulation and tool conceptual processing: the inferior parietal and ventral premotor cortices. The region of the inferior parietal cortex exhibiting differential connectivity to the pMTG is known to underlie execution of complex manual actions required to use tools (Goldenberg and Spatt, 2009) [for related findings with electrical stimulation see (Desmurget *et al.*, 2009)], and has been observed in many tool-related functional neuroimaging studies (Chao *et al.*, 1999, 2002; Beauchamp *et al.*, 2002; Tranel *et al.*, 2005; Mahon *et al.*, 2007; Kemmerer *et al.*, 2008) [for reviews see (Thompson-Schill, 2003; Lewis, 2006; Martin and Simmons, 2008)]. Similarly, the pMTG seed region was differentially correlated with the posterior inferior frontal gyrus and ventral premotor cortex, a region known to store general motor programs for manual movements used in tool manipulation (Goldenberg and Spatt, 2009). Additionally, magnetic disruption of this region with TMS results in selective impairment of tool-word conceptual processing (Cattaneo *et al.*, 2010).

We have learned much about the property contents of the regions described above through functional neuroimaging and neuropsychological studies with lesion patients. Importantly, however, both the performance of lesion patients on neuropsychological tests and healthy control subjects in a brain scanner occur in the context of tasks that require active perceptual/conceptual processing of social and tool stimuli. The fact that the property regions within the social- and tool circuits co-activate during social- and tool tasks might thus have simply reflected the incidental retrieval of properties that are correlated with each other (e.g. how a person looks and what they might be thinking, or how one grasps a key and how a key moves while in use). If the co-activations within these neural networks were due strictly to retrieval of category-correlated property information, then the property regions within the social- and tool knowledge neural networks should have de-coupled when the subjects were no longer engaged in social- and tool-related tasks. As a result, neither neural network should have been observed within task-independent resting-state data. This is precisely not what we observed. Rather, the social–cognitive and tool neural networks persist even when subjects are not engaged in social–cognitive and tool-related information processing.

One potential issue of concern is that the resting-state functional connectivity effects reported here result from unconstrained social- and tool-cognition during the resting scan run. Current findings in the literature, however, provide little support for this possibility. Unlike unconstrained thought, resting-state functional connectivity is based on spontaneous fluctuations in the BOLD signal that are very slow, occurring at ~0.1 Hz or less (Biswal *et al.*, 1995). This may account for recent quantitative demonstrations that unconstrained cognition and context effects account for only a small percent of the variance in spontaneous resting-state BOLD signal fluctuations (Andrews-Hanna *et al.*, 2010a; Grigg and Grady, 2010). Additionally, resting-state functional connectivity among the nodes of large-scale neural networks identified in awake subjects is maintained even under alterations in state of consciousness, including during the induction and emergence from anesthesia (Vincent *et al.*, 2007; Breshears *et al.*, 2010). Collectively these findings provide strong evidence that resting-state functional connectivity effects are not a product of unconstrained cognition, and support our claim that the regions within the social–cognitive and tool use neural networks are persistently coupled, even when subjects are not engaged in social and tool-related cognitive tasks.

The relationship between the social–cognitive and default-mode networks

Because some of the brain regions implicated in the social–cognitive neural network appear to also participate in the default mode network (Raichle *et al.*, 2001; Fox *et al.*, 2005), we assessed the overlap between voxels exhibiting differential functional connectivity to the pSTS seed and those exhibiting differential functional connectivity to a posterior cingulate seed voxel reported previously in the default network literature. There were indeed overlaps, with a subset of the voxels in the posterior cingulate and medial prefrontal cortex, exhibiting stronger functional connectivity to both the posterior cingulate (default-mode) and pSTS

(social–cognitive) seeds than to the pMTG (tool network) seed.

This overlap is not unexpected. The posterior cingulate and medial prefrontal cortex are central both to the social–cognitive neural network and form the 'core' of the default-mode network. In support of this claim, Andrews-Hannah and colleagues (2010b) recently identified constituent sub-networks within the default mode network, inferring the sub-networks' information contents from activation patterns in various cognitive tasks. They concluded that spontaneous BOLD fluctuations in the posterior cingulate and medial prefrontal cortex were more tightly coupled to each other than to other regions in the default network, and that both regions subserve self-relevant (social), affective decisions [also see (Spreng and Grady, 2010)]. And yet, the nodes within the default mode and social–cognitive networks are not identical. As such, it will be important for future studies to explore what factors distinguish those regions of the medial prefrontal cortex and posterior cingulate that are more strongly functionally connected with the other regions in the social–cognitive network than with other nodes in the default network, such as the lateral posterior inferior parietal cortex and the hippocampal formation.

Significance for theories of conceptual knowledge

The results of the present study may have implications for the phenomenon of category-specific deficits. The propagation of noxious interference from a single pathological node within the social–cognitive or tool use circuits may contribute to some category-specific conceptual deficits, in which patients exhibit profound failures of semantic memory for a wide-range of information about a single conceptual category, usually either for animate (animal or social) or inanimate (tool) entities (Capitani *et al.*, 2003). For example, in some patients, tool category-specific deficits can result from damage to the premotor cortex, even though posterior middle temporal and parietal regions remain intact (Tranel *et al.*, 1997). In contrast, other patients may show similar category-specific deficits following damage limited to a different node of the network—the postertior region of the left middle temporal gyrus (Campanella *et al.*, 2010). The persistent functional connectivity among regions in the 'tool' neural network observed in the present study would likely mean that abnormal activity from pathological tissue in one node of the network (i.e. left premotor cortex, left middle temporal gyrus) would constantly propagate to other regions in the network, thus interfering with the ability to retrieve property information from regions that are otherwise intact.

The findings reported here make important contributions to domain-specific theories of semantic memory and knowledge representation. Brain regions identified during conceptual processing of social- and tool categories exhibit task-independent functional connectivity with other regions implicated in social- and tool conceptual processing. This finding lends further evidence to the claim that there exist at least a limited number of domain-specific neural networks that support knowledge of important categories such as tools and social agents.

What might be the functional significance of these dedicated neural networks? One intriguing possibility is that they may support domain-specific conceptual inferences that in turn prime an organism for future action. A persistent coupling between regions supporting perceptual properties associated with a category (e.g. how an entity moves) and regions that support information about the category's non-obvious properties (e.g. what its intentions could be, or how one handles it) might facilitate the sort of quick conceptual inferences that confer evolutionary advantage (New *et al.*, 2007). Our findings demonstrate that analysis of spontaneous BOLD fluctuations can be used to map domain-specific neural systems, thereby extending the application of resting-state analyses beyond broadly defined, domain-general cognitive systems. Perhaps, most importantly, these analyses provide an avenue for investigating both the development of these domain-specific systems in infants and very young children, as well as the breakdown of these systems in patients with neuropsychiatric disorders or limited abilities for task performance (Fox and Greicius, 2010).

SUPPLEMENTARY DATA

Supplementary data are available at *SCAN* online.

Conflict of Interest

None declared.

REFERENCES

Adolphs, R. (2010). What does the amygdala contribute to social cognition? *Annals of the New York Academy of Science*, *1191*, 42–61.

Adolphs, R., Spezio, M. (2006). Role of the amygdala in processing visual social stimuli. *Progress in Brain Research*, *156*, 363–78.

Amodio, D.M., Frith, C.D. (2006). Meeting of minds: the medial frontal cortex and social cognition. *Nature Review Neuroscience*, *7*, 268–77.

Andrews-Hanna, J.R., Reidler, J.S., Huang, C., Buckner, R.L. (2010a). Evidence for the default network's role in spontaneous cognition. *Journal of Neurophysiology*, *104*, 322–35.

Andrews-Hanna, J.R., Reidler, J.S., Sepulcre, J., Poulin, R., Buckner, R.L. (2010b). Functional-anatomic fractionation of the brain's default network. *Neuron*, *65*, 550–62.

Beauchamp, M.S., Lee, K.E., Haxby, J.V., Martin, A. (2002). Parallel visual motion processing streams for manipulable objects and human movements. *Neuron*, *34*, 149–59.

Beauchamp, M.S., Lee, K.E., Haxby, J.V., Martin, A. (2003). FMRI responses to video and point-light displays of moving humans and manipulable objects. *Journal of Cognitive Neuroscience*, *15*, 991–1001.

Bird, G., Silani, G., Brindley, R., White, S., Frith, U., Singer, T. (2010). Empathic brain responses in insula are modulated by levels of alexithymia but not autism. *Brain*, *133*, 1515–25.

Biswal, B., Yetkin, F.Z., Haughton, V.M., Hyde, J.S. (1995). Functional connectivity in the motor cortex of resting human brain using echo-planar MRI. *Magnetic Resonance in Medicine*, *34*, 537–41.

Breshears, J.D., Roland, J.L., Sharma, M., et al. (2010). Stable and dynamic cortical electrophysiology of induction and emergence with propofol anesthesia. *Proceedings of the National Academy of Science USA*, *107*, 21170–5.

Campanella, F., D'Agostini, S., Skrap, M., Shallice, T. (2010). Naming manipulable objects: anatomy of a category specific effect in left temporal tumours. *Neuropsychologia*, *48*, 1583–97.

Capitani, E., Laiacona, M., Mahon, B.Z., Caramazza, A. (2003). What are the facts of semantic category-specific deficits? A critical review of the clinical evidence. *Cognitive Neuropsychology*, *20*, 213–61.

Caramazza, A., Shelton, J.R. (1998). Domain-specific knowledge systems in the brain the animate-inanimate distinction. *Journal of Cognitive Neuroscience*, *10*, 1–34.

Cattaneo, Z., Devlin, J.T., Salvini, F., Vecchi, T., Silvanto, J. (2010). The causal role of category-specific neuronal representations in the left ventral premotor cortex (PMv) in semantic processing. *Neuroimage*, *49*, 2728–34.

Cavanna, A.E., Trimble, M.R. (2006). The precuneus: a review of its functional anatomy and behavioural correlates. *Brain*, *129*, 564–83.

Chao, L.L., Haxby, J.V., Martin, A. (1999). Attribute-based neural substrates in temporal cortex for perceiving and knowing about objects. *Nature Neuroscience*, *2*, 913–9.

Chao, L.L., Weisberg, J., Martin, A. (2002). Experience-dependent modulation of category-related cortical activity. *Cerebral Cortex*, *12*, 545–51.

Cordes, D., Haughton, V.M., Arfanakis, K., et al. (2000). Mapping functionally related regions of brain with functional connectivity MR imaging. *AJNR American Journal of Neuroradiology*, *21*, 1636–44.

Davare, M., Andres, M., Cosnard, G., Thonnard, J.L., Olivier, E. (2006). Dissociating the role of ventral and dorsal premotor cortex in precision grasping. *Journal of Neuroscience*, *26*, 2260–8.

Deen, B., McCarthy, G. (2010). Reading about the actions of others: biological motion imagery and action congruency influence brain activity. *Neuropsychologia*, *48*, 1607–15.

Desmurget, M., Reilly, K.T., Richard, N., Szathmari, A., Mottolese, C., Sirigu, A. (2009). Movement intention after parietal cortex stimulation in humans. *Science*, *324*, 811–3.

Fox, M.D., Greicius, M. (2010). Clinical applications of resting state functional connectivity. *Frontiers in Systems Neuroscience*, *4*, 19.

Fox, M.D., Corbetta, M., Snyder, A.Z., Vincent, J.L., Raichle, M.E. (2006). Spontaneous neuronal activity distinguishes human dorsal and ventral attention systems. *Proceedings of the National Academy of Science USA*, *103*, 10046–51.

Fox, M.D., Snyder, A.Z., Vincent, J.L., Corbetta, M., Van Essen, D.C., Raichle, M.E. (2005). The human brain is intrinsically organized into dynamic, anticorrelated functional networks. *Proceedings of the National Academy of Science USA*, *102*, 9673–8.

Frith, C.D. (2007). The social brain? *Philosophical Transactions of the Royal Society of London B Biological Science*, *362*, 671–8.

Goldenberg, G., Spatt, J. (2009). The neural basis of tool use. *Brain*, *132*, 1645–55.

Greicius, M.D., Krasnow, B., Reiss, A.L., Menon, V. (2003). Functional connectivity in the resting brain: a network analysis of the default mode hypothesis. *Proceedings of the National Academy of Science USA*, *100*, 253–8.

Grigg, O., Grady, C.L. (2010). Task-related effects on the temporal and spatial dynamics of resting-state functional connectivity in the default network. *PLoS ONE*, *5*, e13311.

Grossman, E.D., Jardine, N.L., Pyles, J.A. (2010). fMR-Adaptation Reveals Invariant Coding of Biological Motion on the Human STS. *Frontiers in Human Neuroscience*, *4*, 15.

Haaland, K.Y., Harrington, D.L., Knight, R.T. (2000). Neural representations of skilled movement. *Brain*, *123*(Pt 11), 2306–13.

Hampson, M., Peterson, B.S., Skudlarski, P., Gatenby, J.C., Gore, J.C. (2002). Detection of functional connectivity using temporal correlations in MR images. *Human Brain Mapping*, *15*, 247–62.

Hirschfeld, L.A., Gelman, S.A., editors. (1994). *Mapping the Mind: Domain Specificity in Cognition and Culture*. New York, NY: Cambridge University Press.

Insausti, R., Juottonen, K., Soininen, H., et al. (1998). MR volumetric analysis of the human entorhinal, perhirhinal, and temporopolar cortices. *Am J Neuroradiol*, *19*, 659–71.

Kanwisher, N., Yovel, G. (2006). The fusiform face area: a cortical region specialized for the perception of faces. *Philosophical Transactions of the Royal Society of London B Biological Science*, *361*, 2109–28.

Kanwisher, N., McDermott, J., Chun, M.M. (1997). The fusiform face area: a module in human extrastriate cortex specialized for face perception. *Journal of Neuroscience*, *17*, 4302–11.

Kemmerer, D., Castillo, J.G., Talavage, T., Patterson, S., Wiley, C. (2008). Neuroanatomical distribution of five semantic components of verbs: evidence from fMRI. *Brain and Language*, *107*, 16–43.

Lewis, J.W. (2006). Cortical networks related to human use of tools. *Neuroscientist*, *12*, 211–31.

Mahon, B.Z., Milleville, S.C., Negri, G.A., Rumiati, R.I., Caramazza, A., Martin, A. (2007). Action-related properties shape object representations in the ventral stream. *Neuron*, *55*, 507–20.

Martin, A. (2007). The representation of object concepts in the brain. *Annual Review of Psychology*, *58*, 25–45.

Martin, A., Simmons, W.K. (2008). The structural basis of semantic memory. *Learning and Memory: A Comprehensive Reference*, *3*, 113–130.

New, J., Cosmides, L., Tooby, J. (2007). Category-specific attention for animals reflects ancestral priorities, not expertise. *Proceedings of the National Academy of Science USA*, *104*, 16598–603.

Puce, A., Allison, T., Asgari, M., Gore, J.C., McCarthy, G. (1996). Differential sensitivity of human visual cortex to faces, letterstrings, and textures: a functional magnetic resonance imaging study. *Journal of Neuroscience*, *16*, 5205–15.

Raichle, M.E., MacLeod, A.M., Snyder, A.Z., Powers, W.J., Gusnard, D.A., Shulman, G.L. (2001). A default mode of brain function. *Proceedings of the National Academy of Science USA*, *98*, 676–82.

Ross, L.A., Olson, I.R. (2010). Social cognition and the anterior temporal lobes. *Neuroimage*, *49*, 3452–62.

Schwarzlose, R.F., Baker, C.I., Kanwisher, N. (2005). Separate face and body selectivity on the fusiform gyrus. *Journal of Neuroscience*, *25*, 11055–9.

Seeley, W.W., Menon, V., Schatzberg, A.F., et al. (2007). Dissociable intrinsic connectivity networks for salience processing and executive control. *Journal of Neuroscience*, *27*, 2349–56.

Simmons, W.K., Martin, A. (2009). The anterior temporal lobes and the functional architecture of semantic memory. *Journal of International Neuropsychological Society*, *15*, 645–9.

Simmons, W.K., Reddish, M., Bellgowan, P.S., Martin, A. (2010). The selectivity and functional connectivity of the anterior temporal lobes. *Cerebral Cortex*, *20*, 813–25.

Spreng, R.N., Grady, C.L. (2010). Patterns of brain activity supporting autobiographical memory, prospection, and theory of mind, and their relationship to the default mode network. *Journal of Cognitive Neuroscience*, *22*, 1112–23.

Thompson-Schill, S.L. (2003). Neuroimaging studies of semantic memory: inferring "how" from "where". *Neuropsychologia*, *41*, 280–92.

Tranel, D., Damasio, H., Damasio, A.R. (1997). A neural basis for the retrieval of conceptual knowledge. *Neuropsychologia*, *35*, 1319–27.

Tranel, D., Grabowski, T.J., Lyon, J., Damasio, H. (2005). Naming the same entities from visual or from auditory stimulation engages similar regions of left inferotemporal cortices. *Journal of Cognitive Neuroscience*, *17*, 1293–305.

Vincent, J.L., Kahn, I., Snyder, A.Z., Raichle, M.E., Buckner, R.L. (2008). Evidence for a frontoparietal control system revealed by intrinsic functional connectivity. *Journal of Neurophysiology*, *100*, 3328–42.

Vincent, J.L., Snyder, A.Z., Fox, M.D., et al. (2006). Coherent spontaneous activity identifies a hippocampal-parietal memory network. *Journal of Neurophysiology*, *96*, 3517–31.

Vincent, J.L., Patel, G.H., Fox, M.D., et al. (2007). Intrinsic functional architecture in the anaesthetized monkey brain. *Nature*, *447*, 83–6.

von dem Hagen, E.A., Beaver, J.D., Ewbank, M.P., et al. (2009). Leaving a bad taste in your mouth but not in my insula. *Social Cognitive and Affective Neuroscience*, *4*, 379–86.